A Novel Preformulation Tool to Group Microcrystalline Celluloses Using Artificial Neural Network and Data Clustering

Josephine L. P. Soh[1], Fei Chen[2], Celine V. Liew[1], Daming Shi[2], and Paul W. S. Heng[1,3]

Received July 19, 2004; accepted September 5, 2004

Purpose. To group microcrystalline celluloses (MCCs) using a combination of artificial neural network (ANN) and data clustering.
Methods. Radial basis function (RBF) network was used to model the torque measurements of the various MCCs. Output from the RBF network was used to group the MCCs using a data clustering technique known as discrete incremental clustering (DIC). Rheological or torque profiles of various MCCs at different combinations of mixing time and water:MCC ratios were obtained using mixer torque rheometry (MTR). Correlation analysis was performed on the derived torque parameter $Torque_{max}$ and physical properties of the MCCs.
Results. Depending on the leniency of the predefined threshold parameters, the 11 MCCs can be assigned into 2 or 3 groups. Grouping results were also able to identify bulk and tapped densities as major factors governing water-MCC interaction. MCCs differed in their water retentive capacities whereby the denser Avicel PH 301 and PH 302 were more sensitive to the added water.
Conclusions. An objective grouping of MCCs can be achieved with a combination of ANN and DIC. This aids in the preliminary assessment of new or unknown MCCs. Key properties that control the performance of MCCs in their interactions with water can be discovered.

KEY WORDS: artificial neural network; discrete incremental clustering; microcrystalline cellulose; mixer torque rheometry; preformulation.

INTRODUCTION

Artificial neural network (ANN) is a learning/training system based on a computational technique that can simulate the neurologic processing ability of the human brain (1). ANNs collate knowledge by recognizing patterns and relationships in data and learn through experience or continual training. A comprehensive introduction about ANNs has been reported (2). The ANN learns an approximate nonlinear relationship through a training process. During the training process, the interunit connections are optimized until the error in predictions is minimized and a certain level of accuracy is attained. Once the network is trained, it can be fed with new input information to predict the output. Although ANN methodology is a relatively new field, it has found wide applications in pharmaceutical research, ranging from interpretation of analytical data (data modeling), drug design (molecular modeling), dosage form design (optimization), and pharmacokinetic/dynamic modeling among others (1,3–6).

Analyzing sequences of data is also known as time series data analysis. It aims to find mathematical representations (i.e., finding the inner hidden mappings among data) for modeling data and to forecast future values of the time series variable. Both of these goals require the identification and description of the pattern of observed time series data. Once the pattern is established, it can be interpreted and integrated with other data. Regardless of the depth of understanding and validity of the interpretation (theory) about a given data set, extrapolation can be made to identified patterns for predicting future events and comparing between different patterns. Due to their powerful ability to unravel hidden mappings among data, neural networks can successfully be used in many time series data applications, such as speech synthesis, video surveillance, and finance forecasting. Rheological measurements of microcrystalline celluloses (MCCs) are also forms of time series data and may be analyzed as such.

Neural networks provide linear algorithms capable of representing complex nonlinear mapping, and they can approximate any regular input sequence (7). Their learning ability from training data makes them an important tool for time series analysis. On the other hand, there are different topologies of neural networks that may be used for time series modeling. Among them, radial basis function (RBF) networks have shown considerably better scaling properties, especially when the number of hidden neurons is increased (8). Whereas ANN is useful in modeling and understanding complicated relationships within a given data set, it is inadequate in situations where there is a requisite to achieve some form of objective clustering.

The information derived from ANN alone would not be sufficient to gain an in-depth knowledge of the relationship between different MCCs. To better understand water-MCC interaction, an additional step of data clustering needs to be carried out. Data clustering involves the division of a given data set into smaller groups or clusters, each possessing certain similar characteristics. By clustering, hidden patterns or relationships may be uncovered and is immensely useful in many information retrieval areas including Web mining, medical diagnostics, and marketing analysis.

A novel clustering technique known as discrete incremental clustering (DIC) is also introduced. DIC can determine the optimal number of clusters for a given data set (9) without the need to predefine the number of clusters. This is a distinct advantage as the total number of clusters for a given data set is usually unknown.

Intergrade variability of MCC has been well documented, and much of this was attributed to differences in the source and composition of plant material as well as processing conditions used in its manufacture (10–13). This variability is subsequently reflected as differences in fundamental physical properties of MCCs. These resultant inconsistencies can compromise the control of process parameters during drug product manufacture. The importance of preformulation studies cannot be overemphasized.

The mechanisms by which MCC functions as a spheronization aid of almost unparalleled efficiency have yet to be fully understood, although the key physical properties on the

[1] National University of Singapore, Department of Pharmacy, 18 Science Drive 4, Singapore 117543
[2] Nanyang Technology University, School of Computer Engineering, Nanyang Avenue, Singapore 639798
[3] To whom correspondence should be addressed. (email: phapaulh@nus.edu.sg)

0724-8741/04/1200-2360/0

quality of the pellets formed had been identified (14). Attempts to produce pellets by extrusion-spheronization with very little or no MCC were not encouraging (15). It has thus been generally accepted that MCC is essential for well-controlled pellet production. Other spheronization aids studied (powdered celluloses, low-substituted hydroxypropylcelluloses and pectinic acid) were not of comparable efficiency as MCC in use, compatibility, and quality of pellets formed (16–18).

Inherent variabilities in starting materials may be compensated if better understanding of processing parameters is available. The effects of process parameters, types of extruder, and water content can affect the properties of the pellets formed (19–23).

Mixer torque rheometry (MTR) is a reliable and direct method for assessing mixing resistance of moistened powder masses in granulation studies (24–25). Torque measurements are related to the rheological character or consistency of wet powder masses, which determine whether the mass containing MCC can successfully be spheronized. This is because the performance and functionality of MCC during spheronization is highly dependent on its interaction with water and would be reflected in the consistency of the wet powder mass containing MCC. An optimum range of water:MCC ratios exists for MCC to be effective as a spheronization aid. Outside this range, good quality spheroids cannot be produced. Depending on the grade of MCC used, the range can vary.

The rheological requirements of water:MCC mixes and differences between the MCCs have been reported (26) but were not explored further. There had also been several reported studies relating moisture content and MCC properties in spheronisation (27–29). As torque is related to moisture content and physicochemical properties of MCC, it is imperative that torque measurements will reflect the summative reactions between MCC and moisture; thus, the function and performance of MCC.

This current work will focus on another aspect of water-MCC interaction by powder rheology and seeks to establish a relationship between the rheological profiles and their physical properties using ANN and DIC. In this study, RBF will be applied to model the torque measurements of MCCs. Subsequent to this, DIC will be used to group the MCCs based on the output derived from the RBF network. MCCs with closely related physical properties tend to generate torque profiles that bear close resemblance to each other. Hence, a systematic way of grouping MCCs can be achieved.

MATERIALS AND METHODS

Materials

Eleven MCCs were characterized: Avicel PH 101, Avicel PH 102, Avicel PH 301, Avicel PH 302, Ceolus KG 801 (Asahi, Osaka, Japan); Celex 101 (ISP, Wayne, NJ, USA); Emcocel 50 M, Prosolv 50 M (Mendell, Patterson, NJ, USA); Viva Pur 101 (J. Rettenmaier & Sohne, Holzmulle, Germany); and Pharmacel 101 and Pharmacel 102 (DMV, Veghel, The Netherlands). Prosolv 50 M is a silified grade of MCC and is physically equivalent to Emcocel 50 M. All MCCs were of the same batch as those quoted previously (14). Distilled water was used as the binding liquid.

Physical Characterization of MCCs

Particle size ($\overline{X}$), bulk (ρ_b), and tapped (ρ_t) densities, % crystallinity (X_{cr}), micromeritic parameters ($V_{low\ P}$, $V_{high\ P}$, V_{total}, and ε), and extrusion-spheronization parameters (W_s and $W_{710\ \mu m}$) were previously determined for all MCCs and reproduced in Table I (14).

$V_{low\ P}$ and $V_{high\ P}$ refer to the amount of mercury intruded into the pores at different levels of pressure, and V_{total} is the sum of $V_{low\ P}$ *and* $V_{high\ P}$. ε denotes the percent porosity. W_s refers to the spheronization water sensitivity of MCC, and it is a measure of the tolerance of the MCC to the added moisture. $W_{710\ \mu m}$ refers to the predicted water requirements for producing pellets with a mean size of 710 μm.

Data Modeling Using Artificial Neural Network

An RBF classifier is a three-layer neural network model in which an N-dimensional input vector $\mathbf{x} = (x_1,x_2,...,x_N)$ is broadcasted to each of K neurons in the hidden layer. Each hidden neuron produces an activation function, typically a Gaussian kernel:

$$h_i = \exp\left(-\frac{\|\mathbf{x} - \mathbf{c}_i\|^2}{2\sigma_i^2}\right), \qquad i = 1, 2, \ldots, K \tag{1}$$

where $\mathbf{c}_i$ and σ_i^2 are the center and width of the Gaussian basis function of the ith hidden unit, respectively. The units in the output layer have interconnections with all the hidden units. The jth output neuron has the form:

$$f_j(\mathbf{x}) = \mathbf{w}_j\mathbf{h} = \sum_{i=1}^{K} w_{ij} \exp\left(-\frac{\|\mathbf{x} - \mathbf{c}_i\|^2}{2\sigma_i^2}\right) \tag{2}$$

where $\mathbf{h} = (h_1,h_2,...,h_k)$ is the input vector from the hidden layer, and w_{ij} is the interconnection weight between the jth output neuron and the ith hidden neuron. The architecture of RBF network is shown in Fig. 1.

Training of the ANN was conducted on the torque data measured at different mixing times and water:MCC ratios for the 11 MCCs. An RBF network with 20 hidden neurons was used to model the MCCs where the input vectors were mixing time and water:MCC ratio, and the output vector was torque measurement. Sampling data of a specific MCC was used in training the RBF network where weights of the network were updated iteratively by error back propagation algorithm. After the network was trained for a specific MCC, sampling data of other MCCs were entered to test the mean square errors (MSEs). The results from RBF models were used to calculate the membership function values of DIC clusters.

Data Clustering

In DIC, a cluster grows by the expansion of its kernel, which is controlled by the plasticity parameter, β. The β value governs the extent to which each cluster expands its kernel in order to include a new data point that has been introduced. The β value of a cluster decreases as the cluster expands its kernel. The change of β in a cluster is modeled by the first quadrant of a cosine waveform. Figure 2 shows the decrease of β from an initial value of 0.5.

The tendency parameter (Fig. 3), *TD,* is analogous to a cluster's willingness to grow. It maintains the relevance of a cluster and prevents it from incorporating too many data

TABLE I. Physical Properties[a] of Various MCCs

MCC	$\bar{X}$ (μm)	X_{cr} (%)	$V_{low\ P}$ (ml g^{-1})	$V_{high\ P}$ (ml g^{-1})	V_{total} (ml g^{-1})	ε (%)	ρ_b (g ml^{-1})	ρ_t (g ml^{-1})	$W_{710\ \mu m}$ (% w/w)	W_s (% w/w)
Avicel PH 101	76.53 (0.53)	69.56 (0.95)	1.19 (0.03)	0.35 (0.007)	1.54 (0.03)	65.45 (2.46)	0.31 (0.003)	0.43 (0.003)	36.10 (0.33)	0.068 (0.004)
Avicel PH 102	132.81 (1.95)	69.49 (0.29)	1.22 (0.06)	0.44 (0.044)	1.67 (0.09)	66.92 (5.61)	0.31 (0.002)	0.42 (0.002)	36.19 (0.34)	0.071 (0.002)
Avicel PH 301	73.55 (0.54)	76.37 (7.98)	0.86 (0.06)	0.29 (0.018)	1.14 (0.07)	61.15 (2.88)	0.43 (0.004)	0.56 (0.004)	30.27 (0.24)	0.078 (0.002)
Avicel PH 302	139.41 (1.36)	84.81 (6.99)	0.75 (0.06)	0.30 (0.029)	1.06 (0.08)	60.11 (2.76)	0.46 (0.003)	0.59 (0.003)	29.82 (0.85)	0.076 (0.006)
Ceolus KG 801	66.65 (0.39)	78.61 (8.89)	2.04 (0.05)	0.57 (0.019)	2.61 (0.07)	76.95 (2.55)	0.19 (0.002)	0.30 (0.001)	37.17 (0.75)	0.064 (0.003)
Celex 101	57.18 (0.16)	72.93 (7.28)	1.38 (0.02)	0.45 (0.029)	1.83 (0.005)	68.28 (1.16)	0.28 (0.003)	0.40 (0.001)	38.79 (1.02)	0.062 (0.005)
Emcocel 50 M	70.86 (0.21)	70.38 (1.64)	1.30 (0.02)	0.36 (0.008)	1.66 (0.01)	65.72 (0.33)	0.27 (0.003)	0.38 (0.001)	38.10 (0.29)	0.059 (0.002)
Prosolv 50 M	81.44 (0.54)	70.73 (1.60)	1.45 (0.03)	0.35 (0.051)	1.81 (0.05)	70.00 (1.16)	0.30 (0.003)	0.41 (0.001)	38.25 (1.01)	0.058 (0.004)
Viva Pur 101	68.04 (0.25)	73.52 (3.23)	1.22 (0.07)	0.30 (0.013)	1.52 (0.08)	65.35 (1.93)	0.32 (0.002)	0.45 (0.001)	36.53 (0.83)	0.065 (0.003)
Pharmacel 101	62.24 (0.22)	72.37 (2.53)	1.11 (0.10)	0.49 (0.015)	1.60 (0.11)	62.29 (0.86)	0.30 (0.001)	0.44 (0.001)	37.64 (0.92)	0.062 (0.001)
Pharmacel 102	143.44 (0.66)	73.08 (4.14)	1.22 (0.04)	0.230 (0.036)	1.52 (0.07)	61.55 (3.60)	0.34 (0.003)	0.44 (0.002)	37.50 (0.62)	0.065 (0.001)

MCC, microcrystalline cellulose.
[a] Standard deviations are provided in parentheses.

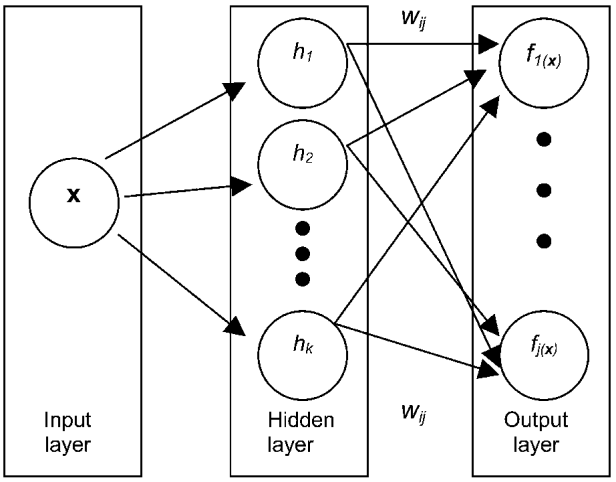

Fig. 1. Architecture of the RBF network.

points that has low fitness (membership function value) to the cluster. *TD* is calculated according to the following equation:

$$TD_{i,j}^{new} = TD_{i,j}^{old} + (A - TD_{i,j}^{old}) \times [1 - \mu_{i,j}(x_i)]^2 \qquad (3)$$

where $\mu_{i,j}$ denotes the membership function of the node *i, j*, and $A = -0.5$. When *TD* is less than or equal to zero, the cluster stops expanding and causes β to become zero.

The input threshold, *IT*, refers to the minimum membership value to decide if an input vector can be assigned to any existing clusters. When the vectors are entered, the first vector will be considered as the cluster center. With this cluster, a new input vector's membership function value is calculated. If it is below the input threshold, the new data will be assigned into the existing cluster. The winner cluster then grows a little according to the predefined β value. In addition, *TD* is calculated to represent the cluster's willingness to "grow." If the new data match the cluster exactly, the cluster keeps its "willingness" to grow. Otherwise, it ceases to grow further. If the membership function value is larger than *IT*, the new input vector becomes a new cluster. The basis parameter set is defined as: $\beta = 0.5$, $IT = 0.9$; the membership function values are based on the results of RBF networks.

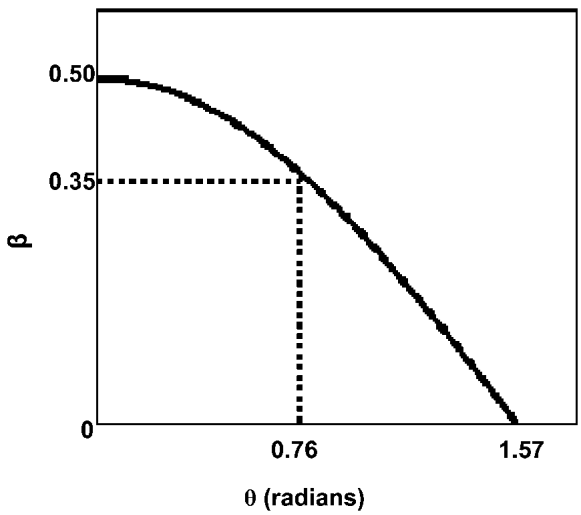

Fig. 2. Modeling of plasticity parameter, β.

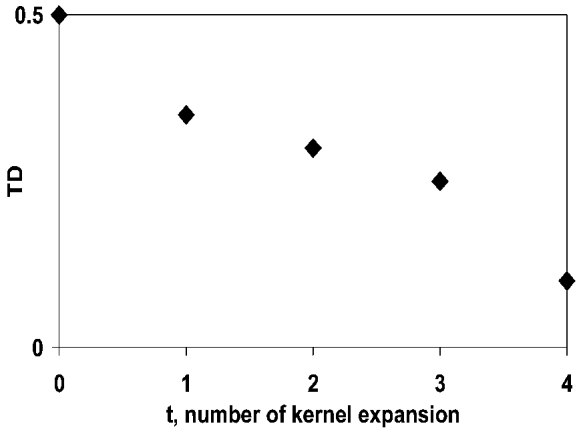

Fig. 3. Dynamics of tendency parameter, *TD*.

MTR Measurements

Degree of Liquid Saturation

Fifteen grams of MCC powder were added into the mixer bowl of the MTR (Caleva Process Solutions Limited, Dorset, England) and mixed for 30 s. The mean torque generated by the dry powder was recorded. Distilled water, corresponding to added water addition of 15% w/w was added to the dry powder at intervals of 30 s for the first 10 additions and at intervals of 60 s for the remaining 9 additions. The entire mixing process was completed in 20 min, and the mean torques generated for 19 additions were recorded. The test was performed in triplicates for each MCC.

Rheological Profiles

Unlike the previous test, water was added only as a bolus dose after the torque generated for the dry powder was recorded. The amounts used ranged from 75% to 220% w/w of MCC powder. All the water was evenly distributed throughout the dry powder while the blades turned. The total mixing time was 46 min for all the MCCs, and respective torque values were logged at regular intervals. Water addition amounting to 200% w/w was too wet to produce any appreciable torque reading for Avicel PH 301 and PH 302; hence, moisture contents equal to and greater than 200% w/w were not investigated for these 2 MCCs. Triplicates were performed for each MCC at all the mixing times and water additions tested.

Statistical Analysis

Correlation analysis was performed using Pearson's correlation analysis (SPSS 12.0 for Windows, SPSS Inc., Chicago, IL, USA). Contour plots were done using SigmaPlot 8.0 (SigmaPlot for Windows, Systat Software, Inc., Richmond, VA, USA).

RESULTS

Data Modeling and Clustering

MSE values obtained from the RBF network (Table II) were subsequently used in the calculation of membership function values required by the DIC method for grouping the MCCs. Two levels of stringency were defined for the DIC parameters, β and *IT*. They are listed as Levels One and Two in Table III with the latter level having a more lenient criterion for the *IT* value.

MTR Measurements

Degree of Liquid Saturation Achieved

Variation of measured torques over a range of water additions was investigated, with the results presented in Fig. 4. The measured torques of all MCC increased as the water content increased, rising to a maximum ($Torque_{max}$) and decreased thereafter when a slurry was produced. This observation was consistent with the different states of liquid saturation (30–31).

Table IV shows the water:MCC ratios required to achieve capillary state of liquid saturation for all the MCCs. These water:MCC ratios corresponded to the $Torque_{max}$ for the respective MCCs. The high-density MCCs, Avicel PH 301 and PH 302, exhibited significantly lower water requirements for achieving capillary saturation (ANOVA, $p < 0.05$). The other nine MCCs were similar in their water requirements at saturation (ANOVA, $p > 0.05$).

Effect of Water:MCC Ratio on Magnitude of $Torque_{max}$

It is observed in Fig. 4 that the high-density MCCs, Avicel PH 301 and PH 302, generated distinctly higher torque values for the same increase in water:MCC ratio (ANOVA,

Table II. Calculated MSE by Modeling the Torque Measurements of MCCs Using RBF

	Training MCC										
Testing MCC	Avicel PH 101	Avicel PH 102	Avicel PH 301	Avicel PH 302	Ceolus KG 801	Celex 101	Emcocel 50 M	Prosolv 50 M	Viva Pur 101	Pharmacel 101	Pharmacel 102
Avicel PH 101	0	0.123	0.676	0.646	0.126	0.102	0.060	0.076	0.196	0.192	0.190
Avicel PH 102	0.123	0	0.574	0.502	0.019	0.046	0.044	0.047	0.039	0.037	0.035
Avicel PH 301	0.919	0.815	0	0.143	0.874	0.965	0.752	0.802	0.739	0.778	0.834
Avicel PH 302	0.887	0.716	0.145	0	0.751	0.874	0.707	0.765	0.629	0.657	0.694
Ceolus KG 801	0.129	0.016	0.614	0.525	0	0.030	0.052	0.064	0.050	0.043	0.032
Celex 101	0.095	0.047	0.709	0.633	0.033	0	0.080	0.089	0.101	0.080	0.065
Emcocel 50 M	0.060	0.045	0.535	0.500	0.054	0.082	0	0.024	0.089	0.087	0.098
Prosolv 50 M	0.074	0.047	0.555	0.525	0.064	0.086	0.024	0	0.077	0.080	0.090
Viva Pur 101	0.196	0.038	0.512	0.433	0.048	0.094	0.089	0.077	0	0.011	0.016
Pharmacel 101	0.187	0.031	0.542	0.452	0.044	0.078	0.083	0.084	0.014	0	0.012
Pharmacel 102	0.182	0.029	0.579	0.478	0.035	0.063	0.094	0.097	0.021	0.014	0

MSE, mean square error; MCC, microcrystalline cellulose; RBF, radial basis function.

Table III. Grouping of MCCs

Group	Level one β = 0.5 *IT* = 0.9	Level two β = 0.5 *IT* = 0.8
1	Celex 101, Ceolus KG 801	Celex 101, Ceolus KG 801, Avicel PH 102
2	Emcocel 50 M, Prosolv 50 M	Emcocel 50 M, Prosolv 50 M
3	Pharmacel 101, Pharmacel 102, Viva Pur 101	Pharmacel 101, Pharmacel 102, Viva Pur 101
—	Avicel PH 101	Avicel PH 101
—	Avicel PH 102	Avicel PH 301
—	Avicel PH 301	Avicel PH 302
—	Avicel PH 302	—

MCC, microcrystalline cellulose.

$p < 0.05$). Statistical analysis also indicated that the non-Avicel MCCs generally exhibited the same rheological profiles when the water additions were varied (ANOVA, $p > 0.05$). Ceolus KG 801, Celex 101, Emcocel 50 M, Prosolv 50 M, and Pharmacel 102 were most comparable to Avicel PH 101 and PH 102 in terms of their rheological profiles (ANOVA, $p > 0.05$).

Particle size did not appear to have an effect on the magnitude of $Torque_{max}$ values, although the large particle size grade of Pharmacel 102 generated a slightly higher torque value than its small particle size counterpart, Pharmacel 101. $Torque_{max}$ values between the three pairs of MCCs (Avicel PH 101 and PH 102; PH 301 and PH 302; Pharmacel 101 and Pharmacel 102) mentioned in the previous paper (32) were not found to be different. Interestingly, these findings did not coincide with those of Rowe and Sadeghnejad (26) who concluded that reduction in the particle size resulted in lower water requirements for attaining $Torque_{max}$. The $Torque_{max}$ obtained was also of a lower magnitude as compared to that produced by a larger particle size grade of MCC. Silification did not have an effect on the $Torque_{max}$ generated.

Effect of Mixing Time and Water:MCC Ratio on Rheological Profiles

Rheological profiles of the MCCs across the entire range of water additions are presented in Fig. 5. At low water:MCC ratios (0.75 and 0.9 ml/g), only Avicel PH 301 and PH 302 generated appreciable torques, because they have lower water tolerance. The comparatively low amounts of water added were sufficient to saturate the interstitial spaces between these MCC particles, leaving some to form liquid films adhering to the particles thus attaining capillary stage of saturation. Between these two MCCs, the larger particle size grade, PH 302, generated a smaller $Torque_{max}$ value than the small particle size counterpart, Avicel PH 301, even though their water requirements at saturation were similar.

At saturation (water:MCC ratio of 1 ml/g), Avicel PH 301 generated a higher torque value than PH 302. This observation corresponded to the findings presented in Fig. 4. Further addition of water (1.25 ml/g and beyond) resulted in slurries or overwetted masses that had much reduced torque values. At intermediate water:MCC ratios (1 to 1.3 ml/g), differences between the remaining 9 MCCs only began to manifest, especially at saturation water:MCC ratios in the region of 1.25 to 1.5 ml/g.

Ceolus KG 801, a low-density, high-porosity MCC grade, exhibited moderate to high torque values at intermediate to high water:MCC ratios (1.25 to 1.75 ml/g). This was attributed to the larger interstitial spaces available for water to reside; therefore, more water was needed to fill the spaces.

Emcocel 50 M and Prosolv 50 M displayed equivalent rheological profiles with moisture regardless of mixing time. Visual examination of the contour plots (Fig. 5) revealed the close resemblance of Ceolus KG 801, Celex 101, and Viva Pur 101 to

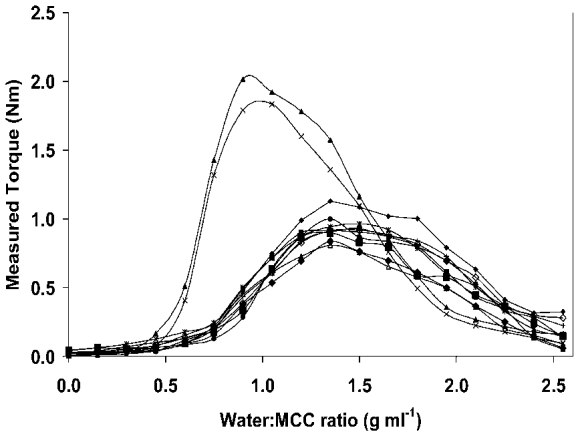

Fig. 4. Variation of measured torque with water: MCC ratio for (◆) Avicel PH 101, (▪) Avicel PH 102, (▲) Avicel PH 301, (✖) Avicel PH 302, (✳) Ceolus KG 801, (✷) Celex 101, (+) Emcocel 50 M, (◇) Prosolv 50 M, (△) Viva Pur 101, (◆) Pharmacel 101, and (■) Pharmacel 102.

Table IV. Saturation Water:MCC Ratio and $Torque_{max}$ for Various MCCs

MCC	MTR measurements[a] Saturation water:MCC ratio	$Torque_{max}$
Avicel PH 101	1.35 (0)	1.129 (0.006)
Avicel PH 102	1.35 (0.150)	0.938 (0.045)
Avicel PH 301	0.95 (0.087)	2.017 (0.027)
Avicel PH 302	0.95 (0.087)	1.847 (0.1)
Ceolus KG 801	1.50 (0)	0.973 (0.109)
Celex 101	1.40 (0.087)	0.999 (0.047)
Emcocel 50 M	1.40 (0.087)	0.934 (0.053)
Prosolv 50 M	1.45 (0.087)	0.928 (0.014)
Viva Pur 101	1.30 (0.087)	0.824 (0.089)
Pharmacel 101	1.40 (0.087)	0.846 (0.055)
Pharmacel 102	1.30 (0.087)	0.912 (0.044)

MCC, microcrystalline cellulose.
[a] Standard deviations are provided in parentheses.

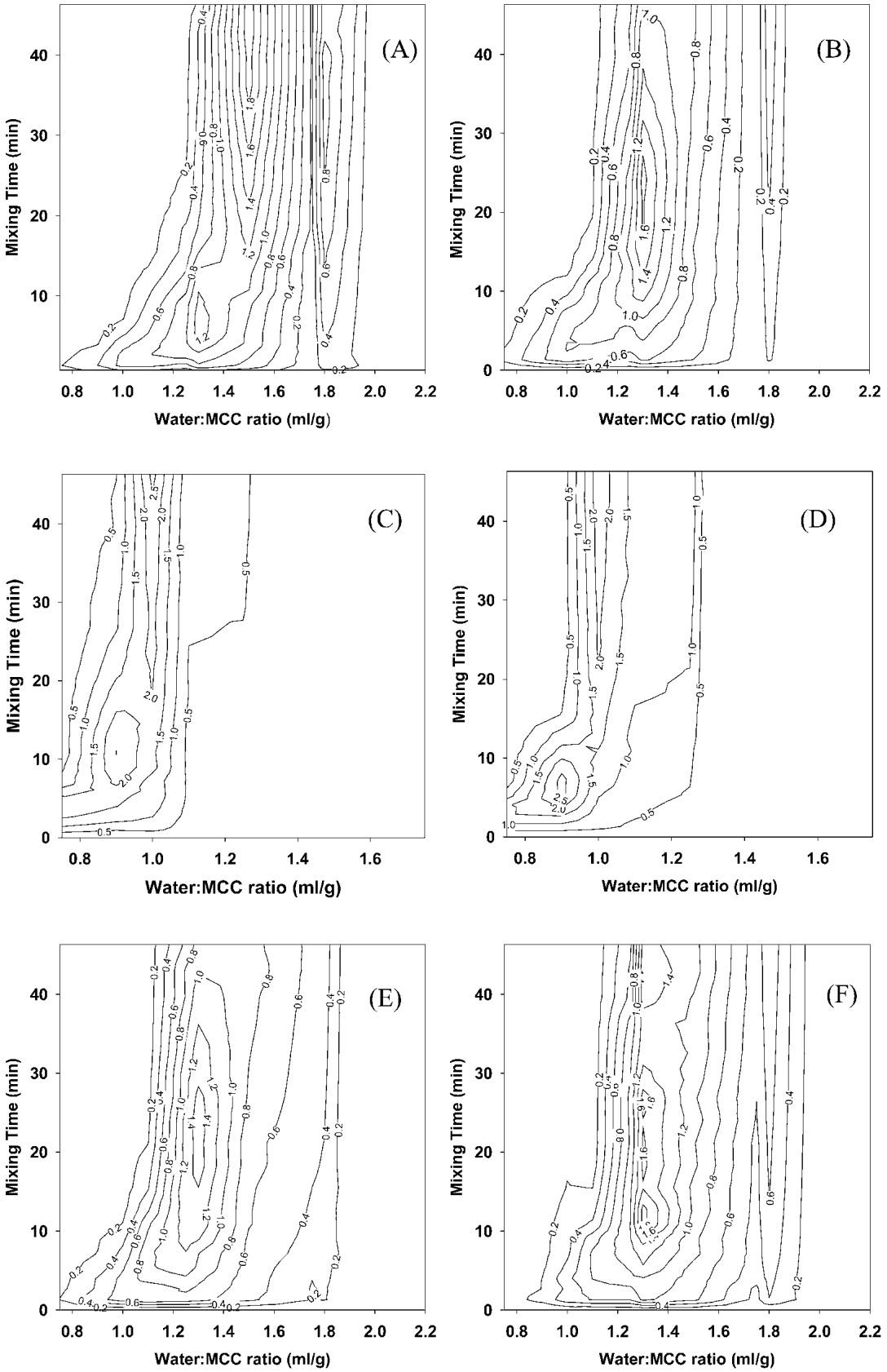

Fig. 5. Effect of water:MCC ratios and mixing times on the torque profiles of (A) Avicel PH 101, (B) Avicel PH 102, (C) Avicel PH 301, (D) Avicel PH 302, (E) Ceolus KG 801, (F) Celex 101, (G) Emcocel 50M, (H) Prosolv 50M, (I) Viva Pur 101, (J) Pharmacel 101, and (K) Pharmacel 102. Torque values in [Nm] Newton Meters.

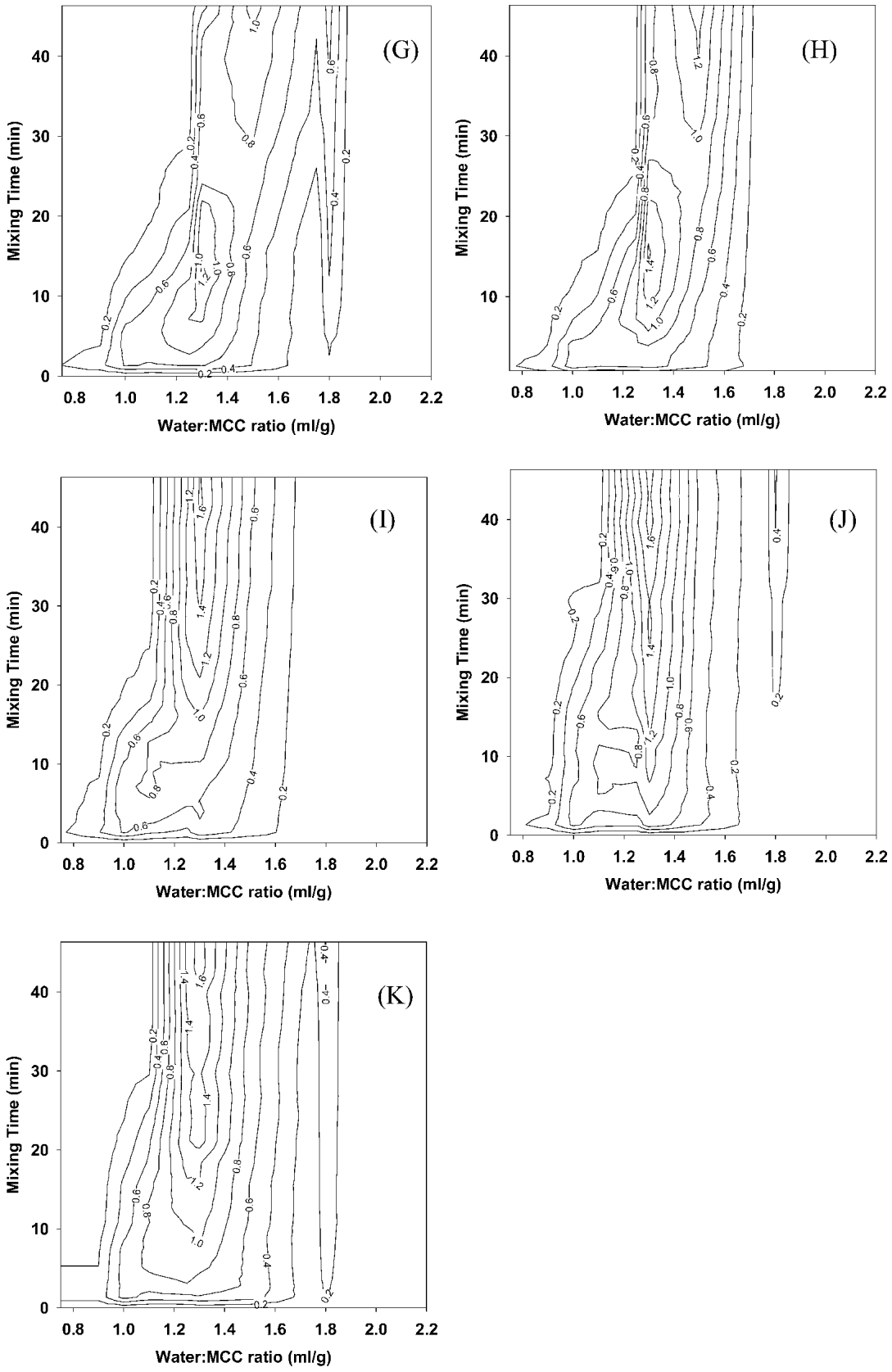

Fig. 5. Continued.

Avicel PH 102 across the entire range of water concentrations tested.

Correlation Analysis

Crystallinity, bulk and tapped densities, and W_s were positively correlated with $\text{Torque}_{\max}$ (Pearson's correlation coefficient: $r = 0.652$, p = 0.03; $r = 0.811$, p = 0.002; $r = 0.798$, p = 0.003; $r = 0.838$, p = 0.001) at the 0.05 level (2-tailed). The $V_{low\ P}$, V_{total}, and $W_{710\ \mu m}$ showed negative correlations (Pearson's correlation coefficient: $r = -0.615$, p = 0.044; $r = -0.608$, p = 0.047; $r = -0.944$, p = 0.000). This was not surprising as higher shear forces were needed to drive the mixer blades through wetted masses. Consequently, the torques generated at saturation for Avicel PH 301 and PH 302 were almost double those of the other MCCs.

DISCUSSION

On their own, the MSE values have limited usefulness. They merely serve as indicators of the relative degree of similarity between any random pair of MCCs. Moreover, these results only allow one-to-one comparisons between any two randomly selected MCCs. The numerical values obtained are arbitrary and should not be compared across the board to yield any meaningful conclusions. A MSE value of zero indicates the lack of difference. The smaller the MSE value, the more similar are the pair of MCCs compared.

Clustering results can be explained in terms of the physical properties of the MCCs. Although Celex 101 and Ceolus KG 801 were in the same group (Level One, Group 1), close examination of their measured physical properties revealed little similarity between them. This meant that each property affects the degree of water-MCC interaction differently, albeit in varying extents. For the members of this group, their differences were somewhat balanced out, thus resulting in them having similar rheological behaviors when moistened. This discussion also holds true for the MCCs in Group 2 (Level One), as Emcocel 50 M and Prosolv 50 M also differed in several physical aspects. Silification was not found to affect granulation and densification of the wet granulates significantly, although Prosolv 50 M had higher compressibilities (higher bulk and tapped density) due to better flow properties imparted by the silicon dioxide. More importantly, it meant that the intrinsic ability of MCC to absorb and redistribute water was not affected by the presence of flow-enhancing agents such as silicon dioxide.

Under the first stringency level, the four Avicel MCC grades were present as single entities, and even under a reduced level of stringency (Level Two), three of them remained as distinct entities and were ungrouped. This meant that their rheological profiles were dissimilar to the other MCCs used in this current study. Nonetheless, these results indicated the effects of the physical properties of MCCs on their interaction with water. The major differences between Avicel PH 101 and PH 102 was in their particle size and bulk and tapped densities. These disparities were sufficient to separate them. Similarly, Avicel PH 301 and PH 302 differed in their particle size, crystallinity, and bulk and tapped densities. The two high-density MCCs, Avicel PH 301 and PH 302, showed different rheological properties but were similar in their lower capacities to accommodate the added water in their interstitial spaces and thus were more readily saturated. Better packing (as indicated by higher bulk and tapped densities) and lower pore volumes (indicated by micromeritic parameters) compromised the interstitial spaces available for the added water to reside and were believed to be responsible for their reduced water tolerance. This also implied that Avicel PH 301 and PH 302 had higher water sensitivities and were less able to accommodate changes in water content during granulation. With more MCCs introduced, it may be possible that they are similar to those single MCC entities in this study to form a new group. As such, this model could be used to classify the rheological properties of any newly introduced MCC.

For ascertaining the influence of particle size, Viva Pur 101, Pharmacel 101, and Pharmacel 102 were examined. Despite being obtained from different suppliers, Viva Pur 101 and Pharmacel 102 had strikingly similar physical properties: their only distinction being particle size. On the contrary, the two Pharmacel grades were markedly different in several aspects (Table I). As such, the influence of particle size would be more aptly demonstrated by comparing Viva Pur 101 and Pharmacel 102 instead. Yet, regardless of the stringency of DIC parameters applied, all the three MCCs were in the same group.

When the stringency of the DIC parameters was reduced to Level Two, Avicel PH 102 was assigned into Group 1. Close examination of the physical properties of Celex 101 and Avicel PH 102 showed that these two MCCs rank very similarly in the $V_{low\ P}$, ε and kawakita constant ($1/b$) values. These parameters refer to the pore volumes and the cohesiveness of the MCC particles. Thus, these parameters were considerably more important in water uptake and distribution. Movement of the added water was also influenced by the densification of granulates during mixing. This finding suggests that Avicel PH 102 and Celex 101 were similar. Further reduction in the stringency of the DIC parameters ($IT < 0.8$), resulted in the 11 MCCs being divided into 2 groups: the high-density Avicel PH 301 and PH 302 in one group and the remaining 9 MCCs in another group. Having considered all the above observations, bulk and tapped densities were believed to exert major influences on the rheological behaviors of the MCCs, corroborating with the results obtained by correlation studies.

CONCLUSIONS

The multiplicity of physicochemical properties of MCCs affects their functionality as spheronization aids and complicates grouping attempts of MCCs based solely on any individual physicochemical property. The combination of ANN and DIC offers the opportunity for clustering MCCs into discrete groups that possess equivalent or comparable performance; thus, providing a basis for suggesting interchangeability among MCCs within the same group. This is especially advantageous for formulation scientists during the preformulation and optimization phases of product development. Additionally, the findings from this study demonstrated the strong influences of bulk and tapped densities in governing water-MCC interactions. Evidently, this phenomenon involves an interplay of many factors, each contributing to varying extents.

The acquired knowledge can further be extended to explore the relationship between the quality of formed sphe-

roids and the rheological profiles of MCCs. Thereafter, extrapolation of the clustering results will be able to predict the performance of these MCCs in spheroid production. This will not only improve process optimization and quality control but, more significantly, opens up opportunities for the development of newer MCCs with superior qualities and allows the potential of any newly introduced MCC to be assessed as an alternative to the existing grades.

REFERENCES

1. A. S. Achanta, J. G. Kowalski, and C. T. Rhodes. Artificial neural networks: implications for pharmaceutical sciences. *Drug Dev. Ind. Pharm.* **21**:119–155 (1995).
2. S. Agatonovic-Kustrin and R. Beresford. Basic concepts of artificial neural network (ANN) modeling and its application in pharmaceutical research. *J. Pharmaceut. Biomed.* **22**:717–727 (2000).
3. A. S. Hussain, X. Yu, and R. D. Johnson. Application of neural computing in pharmaceutical product development. *Pharm. Res.* **8**:1248–1252 (1991).
4. E. Murtoniemi, P. Merkku, P. Kinnunen, K. Leiviskä, and J. Yliruusi. Effect of neural network topology and training end point in modelling the fluidized bed granulation process. *Int. J. Pharm.* **110**:101–108 (1994).
5. M. Gasperlin, L. Tusar, M. Tusar, J. Kristl, and J. Smid-Korbar. Lipophilic semisolid emulsion systems: viscoelastic behaviour and prediction of physical stability by neural network modeling. *Int. J. Pharm.* **168**:243–254 (1998).
6. K. Takayama, M. Fujikawa, and T. Nagai. Artificial neural network as a novel method to optimize pharmaceutical formulations. *Pharm. Res.* **16**:1–6 (1999).
7. C. M. Bishop. Improving the generalization properties of radial basis function neural networks. *Neural Comput.* **3**:579–588 (1991).
8. A. Robel. Scaling properties of neural networks for the prediction of time series. In: *Proceedings of the 6th IEEE Workshop on Neural Networks for Signal Processing*, Kyoto, Japan, 1996, pp. 190–199.
9. W. L. Tung and C. Quek. GenSoFNN: A generic self-organizing fuzzy neural network. *IEEE Trans. Neural Netw.* **13**:1075–1086 (2002).
10. M. Whiteman and R. J. Yarwood. Variations in the properties of microcrystalline cellulose from different sources. *Powder Tech.* **54**:71–74 (1998).
11. M. Landin, R. Martinez-Pacheo, J. L. Gomez-Amoza, C. Souto, A. Concheiro, and R. C. Rowe. Effect of batch variation and source of pulp on the properties of microcrystalline cellulose. *Int. J. Pharm.* **91**:133–141 (1993).
12. R. C. Rowe, A. G. McKillop, and D. Bray. The effect of batch and source variation in the crystallinity of microcrystalline cellulose. *Int. J. Pharm.* **101**:169–172 (1994).
13. M. D. Parker, P. York, and R. C. Rowe. Binder-substrate interactions in wet granulation. 3: The effect of excipient source variation. *Int. J. Pharm.* **80**:179–190 (1992).
14. P. W. S. Heng and O. M. Y. Koo. A study of the effects of the physical characteristics of microcrystalline cellulose on performance in extrusion-spheronisation. *Pharm. Res.* **18**:480–487 (2001).
15. A. W. Basit, J. M. Newton, and L. F. Lacey. Formulation of ranitidine pellets by extrusion-spheronization with little or no microcrystalline cellulose. *Pharm. Dev. Tech.* **4**:499–505 (1999).
16. H. Lindner and P. Kleinbudde. Use of powdered cellulose for the production of pellets by extrusion/spheronisation. *J. Pharm. Pharmacol.* **46**:2–7 (1994).
17. P. Kleinbudde. Application of low substituted hydroxypropylcellulose (L-HPC) in the production of pellets using extrusion/spheronisation. *Int. J. Pharm.* **96**:119–128 (1993).
18. L. Tho, S. A. Sande, and P. Kleinbudde. Pectinic acid, a novel excipient for production of pellets by extrusion/spheronization: preliminary studies. *Eur. J. Pharm. Biopharm.* **54**:95–99 (2002).
19. L. Baert, H. Vermeersch, J. P. Remon, J. Smeyers-Verbeke, and D. L. Massart. Study of the parameters important in the spheronisation process. *Int. J. Pharm.* **96**:225–229 (1993).
20. J. M. Newton, S. R. Chapman, and R. C. Rowe. The influence of process variables on the preparation and properties of spherical granules by the process of extrusion-spheronisation. *Int. J. Pharm.* **120**:101–109 (1995).
21. L. Baert, J. P. Remon, J. A. C. Elbers, and E. M. G. Van Bommel. Comparison between a gravity feed extruder and a twin screw extruder. *Int. J. Pharm.* **99**:7–12 (1993).
22. J. F. Pinto, G. Buckton, and J. M. Newton. The influence of four selected processing and formulation factors on the production of spheres by extrusion and spheronisation. *Int. J. Pharm.* **83**:187–196 (1992).
23. C. Lustig-Gustafsson, J. H. Kaur, F. Podczeck, and J. M. Newton. The influence of water content and drug solubility on the formulation of pellets by extrusion and spheronisation. *Eur. J. Pharm. Sci.* **8**:147–152 (1999).
24. A. Johansen, T. Schaefer, and H. G. Kristensen. Evaluation of melt agglomeration properties of polyethylene glcols using a mixer torque rheometer. *Int. J. Pharm.* **183**:155–164 (1999).
25. R. Chatlapalli and B. D. Rohera. Rheological characterization of diltiazem HCl/cellulose wet masses using a mixer torque rheometer. *Int. J. Pharm.* **175**:47–59 (1998).
26. R. C. Rowe and G. R. Sadeghnejad. The rheology of microcrystalline powder/water mixes using a mixer torque rheometer. *Int. J. Pharm.* **38**:227–229 (1987).
27. R. M. Iyer, L. L. Augsburger, and D. G. Pope. Extrusion/spheronisation-effect of moisture content and spheronisation time on pellet characteristics. *Pharm. Dev. Tech.* **1**:325–331 (1996).
28. K. E. Fielden, J. M. Newton, and R. C. Rowe. Influence of moisture content on spheronisation of extrudate processed by ram extruder. *Int. J. Pharm.* **97**:79–92 (1993).
29. D. Bains, S. L. Boutell, and J. M. Newton. Influence of moisture content on the preparation of spherical granules of barium sulphate and MCC. *Int. J. Pharm.* **69**:233–237 (1991).
30. M. D. Parker, R. C. Rowe, and N. G. Upjohn. Mixer Torque Rheometry - A method for quantifying the consistency of wet granulation. *Pharm. Tech. Int.* **2**:50–62 (1990).
31. D. M. Newitt and J. M. Conway-Jones. A contribution to the theory and practice of granulation. *Trans. Int. Chem. Eng.* **36**: 422–442 (1958).
32. P. W. S. Heng, C. V. Liew, and J. L. P. Soh. Pre-formulation studies on moisture absorption in microcrystalline cellulose using differential thermo-gravimetric analysis. *Chem. Pharm. Bull. (Tokyo)* **52**:384–390 (2004).